Scattering of time-harmonic antiplane shear waves in magnitoelectroelastic materials

Yonko D. Stoynov

Citation: AIP Conf. Proc. **1497**, 53 (2012); doi: 10.1063/1.4766766
View online: http://dx.doi.org/10.1063/1.4766766
View Table of Contents: http://proceedings.aip.org/dbt/dbt.jsp?KEY=APCPCS&Volume=1497&Issue=1
Published by the American Institute of Physics.

Scattering of time-harmonic antiplane shear waves in magnitoelectroelastic materials

Yonko D. Stoynov

Faculty of Applied Mathematics and Informatics, Technical University of Sofia.

Abstract: In this paper the dynamic behavior of cracked magnetoelectroelastic materials under antiplane mechanical and inplane electric and magnetic load is investigated. The boundary value problem for the coupled system of governing equations is reduced to a non-hypersingular traction boundary integral equation using generalization of the well-known J-integrals in elastostatics.

Software based on the Boundary Integral Equation Method (BIEM) is developed using FORTRAN. Validation with the results for piezoelectric materials obtained by the dual integral equation method is given. The numerical examples show the dependence of the Stress Intensity Factor (SIF) on the normalized frequency of the incident wave for different materials and different boundary conditions.

Keywords: magnetoelectroelastic medium, anti – plane crack, BIEM, SIF.

PACS: 02.30.Jr, 02.70.Pt, 75.50.Gg, 77.84.Lf, 77.84.Dy

1. Introduction

Magnetoelectroelastic materials (MEEM), possessing magnetoelectric coupling property, have increasing applications in modern engineering structures. Since these materials are brittle, they are sensitive to cracks. During the service life they are subjected to external loads, which may lead to crack extension and eventually to disintegration of the materials and/or loosing of their functional properties. Hence fracture mechanics analysis has an important role in the design of the MEEM.

One of the basic issues of the fracture mechanics of the MEEM is the electromagnetic boundary conditions along the crack. For the piezoelectric materials there are two types of idealized boundary conditions-electrically permeable and impermeable. These assumptions will be generalized to MEEM to address the magnetically permeable and impermeable cracks (see [1]).

The objective of this paper is to consider MEEM, subjected to time-harmonic loads and give numerical results for different boundary conditions along crack faces.

2. Statement of the problem

Let's consider linear MEE medium subjected to an external electromagnetic field. The constitutive equations, which give relation between the mechanical, electrical and magnetic field can be found in [2-3]. We assume that the medium is transversely isotropic with an axis of symmetry along Ox_3 direction of a rectangular coordinate system $Ox_1x_2x_3$. The medium is subjected to an external antiplane mechanical, and inplane electric and magnetic load with respect to the plane Ox_1x_2. The electric and magnetic fields are potential and the problem is two-dimensional (the material properties are the same in all planes perpendicular to the axis of symmetry). The constitutive equations in this case are:

$$\begin{aligned}
\sigma_{i3} &= c_{44}u_{3,i} + e_{15}\varphi_{,i} + q_{15}\psi_{,i} \\
D_i &= e_{15}u_{3,i} - \varepsilon_{11}\varphi_{,i} - d_{11}\psi_{,i} \qquad (1) \\
B_i &= q_{15}u_{3,i} - d_{11}\varphi_{,i} - \mu_{11}\psi_{,i}.
\end{aligned}$$

Applications of Mathematics in Engineering and Economics (AMEE '12)
AIP Conf. Proc. 1497, 53-60 (2012); doi: 10.1063/1.4766766

Here c_{44} is the elastic module, e_{15} is the piezoelectric coefficient, q_{15} is the piezomagnetic coefficient, ε_{11} is the dielectric permittivity, μ_{11} is the magnetic permeability, d_{11} is the magnetoelectric coefficient, u_3 is the mechanical displacement, φ and ψ are electric and magnetic potential respectively, σ_{i3} is the mechanical stress, D_i is the inplane electrical displacement, B_i is the inplane magnetic induction, $i=1,2$ and comma means differentiation. Applying the equation of motion, the equations of Maxwell and (1) we obtain the system of governing equations in the absence of body forces, electric charges and current densities:

$$\begin{aligned} &c_{44}\Delta u_3 + e_{15}\Delta\varphi + q_{15}\Delta\psi = \rho\frac{\partial^2 u_3}{\partial t^2} \\ &e_{15}\Delta u_3 - \varepsilon_{11}\Delta\varphi - d_{11}\Delta\psi = 0 \\ &q_{15}\Delta u_3 - d_{11}\Delta\varphi - \mu_{11}\Delta\psi = 0, \end{aligned} \tag{2}$$

where Δ is a two-dimensional Laplace operator and ρ is the density. Eliminating $\Delta\varphi$ and $\Delta\psi$ from the second and third equation of (2) and substituting in the first one we obtain a reduced equation for the mechanical displacement. This equation is hyperbolic. Therefore the system (2) is hyperbolic. In the case of time-harmonic load with a given frequency ω the system (2) can be written in the following way:

$$\begin{aligned} &c_{44}\Delta u_3 + e_{15}\Delta\varphi + q_{15}\Delta\psi + \rho\omega^2 u_3 = 0 \\ &e_{15}\Delta u_3 - \varepsilon_{11}\Delta\varphi - d_{11}\Delta\psi = 0 \\ &q_{15}\Delta u_3 - d_{11}\Delta\varphi - \mu_{11}\Delta\psi = 0, \end{aligned} \tag{3}$$

where u_3, φ and ψ depend only on $x=(x_1,x_2)$. We can substitute $\Delta\varphi$ and $\Delta\psi$ from the second and third equation of (2) in the first one and obtain an elliptic equation. Therefore the system (3) is elliptic. Using a generalized tensor of elasticity $C_{iJKl}, i,l=1,2;\ J,K=3,4,5$:

$$C_{i33l}=\begin{cases} c_{44}, i=l \\ 0, i\neq l \end{cases}, C_{i34l}=C_{i43l}=\begin{cases} e_{15}, i=l \\ 0, i\neq l \end{cases},\ C_{i35l}=C_{i53l}=\begin{cases} q_{15}, i=l \\ 0, i\neq l \end{cases},$$

$$C_{i44l}=\begin{cases} -\varepsilon_{11}, i=l \\ 0, i\neq l \end{cases}, C_{i45l}=C_{i54l}=\begin{cases} -d_{11}, i=l \\ 0, i\neq l \end{cases}, C_{i55l}=\begin{cases} -\mu_{11}, i=l \\ 0, i\neq l \end{cases},$$

a generalized displacement vector $u_J=(u_3,\varphi,\psi)$, $J=3,4,5$ and a generalized stress tensor $\sigma_{iJ}=(\sigma_{i3},D_i,B_i)$, $i=1,2,\ J=3,4,5,$ the governing equations have the compact form:

$$\sigma_{iJ,i} + \rho_{JK}\omega^2 u_K = 0, \tag{4}$$

where $i=1,2,\ J,K=3,4,5,\ \rho_{JK}=\begin{cases} \rho, J=K=3 \\ 0, J,K=4\, or\, 5 \end{cases}$ and we assume summation for repeated indexes.

The material is subjected to an incident wave. The interaction of the incident wave with the crack $\Gamma=\Gamma^+\cup\Gamma^-$, where Γ^+ is the upper bound and Γ^- is the lower bound of the crack, induces scattered waves. The total wave field at any point can be found as a superposition of the incident and scattered wave fields:

$$u_J = u_J^{in} + u_J^{sc}$$

and

$t_J = t_J^{in} + t_J^{sc}$.

Here u_J is the total generalized displacement, t_J is the total generalized traction defined as $t_J = \sigma_{iJ} n_i$, where $n = (n_1, n_2)$ is the normal vector to the crack, u_J^{in} and t_J^{in} are the displacement and traction of the incident wave field and u_J^{sc} and t_J^{sc} are the displacement and traction of the scattered by the crack wave field. The incident wave field is known (see [4]). The scattered field has to be determined so that the Sommerfeld's radiation condition at infinity and the boundary conditions at the crack faces are satisfied.

We will consider the following types of electromagnetic boundary conditions:

Electrically impermeable and magnetically permeable crack (type I) In this case the crack is free of mechanical tractions and surface charges, but continuity of the magnetic potential is assumed:

$t_3\big|_\Gamma = 0$, $t_4\big|_\Gamma = 0$, $t_5\big|_\Gamma = B^{cr}$, $\Delta\psi = \psi^+ - \psi^- = 0$, $B^{cr} = B^+ = B^-$. Here ψ^+ and B^+ are the magnetic potential and the normal component of the magnetic induction at Γ^+, ψ^- and B^- are the magnetic potential and the normal component of the magnetic induction at Γ^- and B^{cr} is the normal component of the magnetic induction inside the crack. Therefore the boundary conditions on Γ can be written as:

$t_J^{sc} = -t_J^{in}, J = 3,4$, $t_5^{sc} = B^{cr} - t_5^{in}$.

Electrically permeable and magnetically impermeable crack (type II) The crack is free of mechanical tractions and surface currents, but continuity of the electric potential is assumed:

$t_3\big|_\Gamma = 0$, $t_4\big|_\Gamma = D^{cr}$, $t_5\big|_\Gamma = 0$, $\Delta\varphi = \varphi^+ - \varphi^- = 0$, $D^{cr} = D^+ = D^-$. Here φ^+ and D^+ are the electric potential and the normal component of the electric displacement at Γ^+, φ^- and D^- are the electric potential and the normal component of the electric displacement at Γ^- and D^{cr} is the normal component of the electric displacement inside the crack. Therefore the boundary conditions on Γ can be written as:

$t_J^{sc} = -t_J^{in}, J = 3,5$, $t_4^{sc} = D^{cr} - t_4^{in}$.

Fully impermeable crack (type III) The crack faces are free of mechanical traction, surface charges and currents:

$t_3\big|_\Gamma = 0$, $t_4\big|_\Gamma = 0$, $t_5\big|_\Gamma = 0$ or $t_J^{sc} = -t_J^{in}, J = 3,4,5$ on Γ.

Fully permeable crack (type IV) The crack is free of mechanical traction, but continuity of electric and magnetic potentials is assumed:

$t_3\big|_\Gamma = 0$, $t_4\big|_\Gamma = D^{cr}$, $t_5\big|_\Gamma = B^{cr}$.

We will solve the respective boundary value problem for (4) transforming it into an equivalent integro – differential system of equations on the crack Γ and then solve this system numerically.

3. Boundary integral equation

It can be proven that if $u_J(x_1, x_2, x_3)$ satisfies (4), the following equality is fulfilled:

$$\oint\!\!\oint_S [\frac{1}{2}(\sigma_{Ji} u_{J,i} - \rho_{JK}\omega^2 u_J u_K)\delta_{js} - \sigma_{Jj} u_{J,s}] n_j dS = 0\,, \qquad (5)$$

where S is a closed surface in the space, enclosing domain D, the vector $n = (n_1, n_2, n_3)$ is an outer normal vector to S, δ_{js} is the Kronecker's delta. The equality (5) can be considered as a generalization of the well-known J-integrals in elastostatics (see [5-6]). Following Wang and Zahng [7] for the piezoelectric case we obtain the BIE:

$$t_J^{in} = -C_{iJKl}(x) n_i(x) \int_{\Gamma^+} [(\sigma^*_{\eta JK}(x,y,\omega)\Delta u_{J,\eta}(y,\omega) - \rho_{QJ}\omega^2 u^*_{QK}(x,y,\omega)\Delta u_J(y,\omega))\delta_{\lambda l}$$
$$-\sigma^*_{\lambda JK}(x,y,\omega)\Delta u_{J,l}(y,\omega)] n_\lambda(y) d\Gamma(y). \qquad (6)$$

Here u^*_{QK} is the fundamental solution, $\sigma^*_{iPK} = C_{iPMl} u^*_{MK,l}$, t_J^{in} is the incident plane wave and $\Delta u_J = u_J\Big|_{\Gamma^+} - u_J\Big|_{\Gamma^-}$ are the unknown COD. The fundamental solution and the incident plane wave can be found in [4]. We reduce the BIE (6) to a system of linear equations and solve it numerically. The traction field in every point $x \in R^2 \setminus \Gamma$ can be found by the corresponding representation formula (see [4]). The stress concentration near crack tips is computed using the formula: $K_{III} = \lim_{x_1 \to \pm c} t_3 \sqrt{2\pi(x_1 \mp c)}$, where c is the half-length of the crack.

4. Numerical realization

The numerical solution scheme follows the procedure developed in Rangelov et al. [8] A FORTRAN program is created and the numerical results are obtained using PC – Core 2 Duo CPU E8500, 3.16GHz and 2.53GHz, 3GB RAM. The MEE material that we used is piezoelectric/piezomagnetic composite $BaTiO_3 / CoFe_2O_4$. The material constants of the used materials can be found in [4].

4.1 Validation studies

We validated our numerical tool with the results of Zhou and Wang [9] for a fully permeable crack. The crack is horizontal along the Ox_1 axis and occupies the interval *(-c,c)*, where *c=5mm.* It is divided into 7 and 15 boundary elements (BE). The results obtained with a mesh of 7 and 15 BE are compared with those of Zhou and Wang. The comparison is given in Fig.1. We see good coincidence of the results.

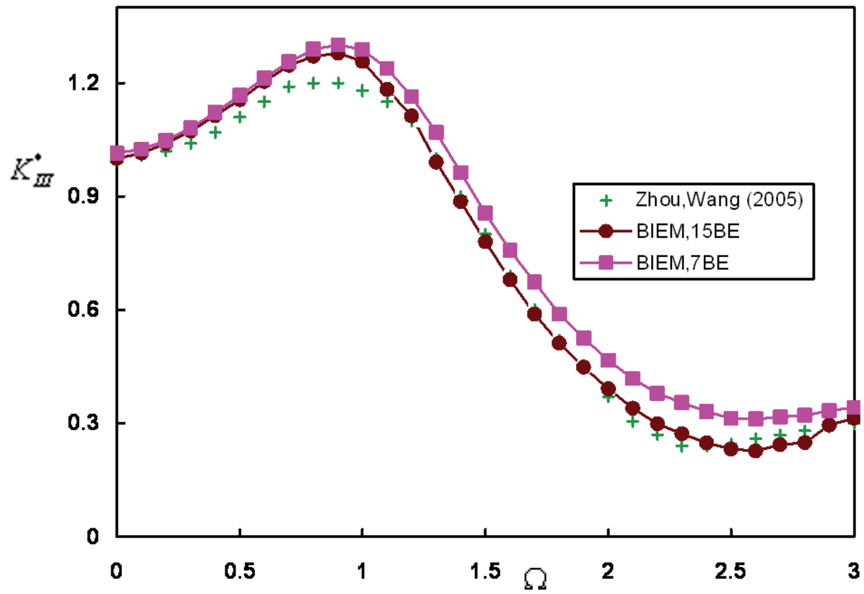

FIGURE 1. The normalized SIF $K_{III}^* = \dfrac{K_{III}}{t_3^{in}\sqrt{\pi c}}$ versus the normalized frequency $\Omega = c\sqrt{\rho \tilde{a}^{-1}}\omega$ for composite material, where $\tilde{a} = \tilde{c}_{44} + \dfrac{\tilde{e}_{15}^2}{\tilde{\varepsilon}_{11}}$, $\tilde{c}_{44} = c_{44} + \dfrac{(q_{15})^2}{\mu_{11}}$, $\tilde{e}_{15} = e_{15} - \dfrac{d_{11}q_{15}}{\mu_{11}}$, $\tilde{\varepsilon}_{11} = \varepsilon_{11} - \dfrac{(d_{11})^2}{\mu_{11}}$.

Another test with the results of Narita and Shindo [10] is presented in Fig. 2. The crack is fully impermeable and the material is $BaTiO_3$. We see very close coincidence of the results.

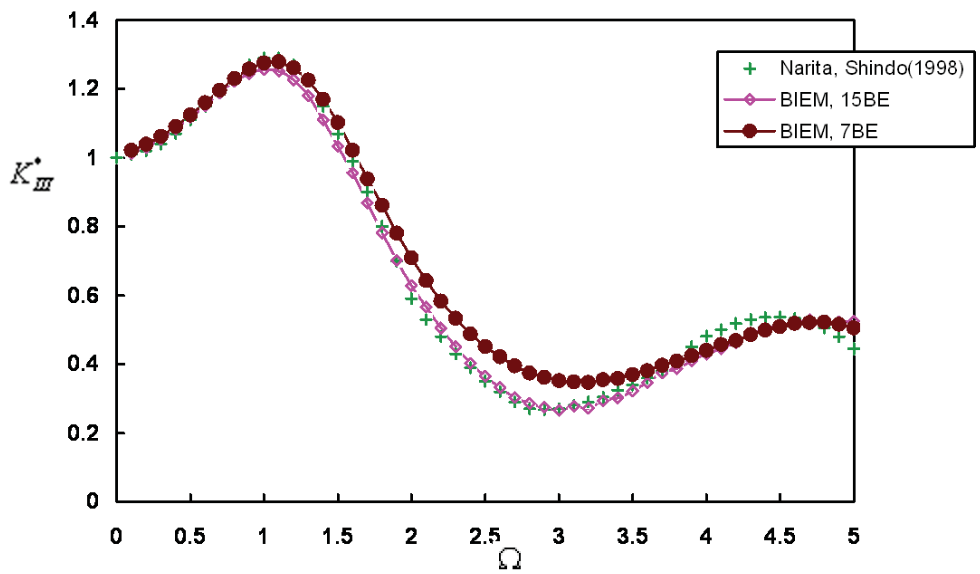

FIGURE 2. The normalized SIF $K_{III}^* = \dfrac{K_{III}}{t_3^{in}\sqrt{\pi c}}$ versus the normalized frequency $\Omega = c\sqrt{\rho c_{44}^{-1}}\omega$ for the piezoelectric material $BaTiO_3$.

4.2 Parametric studies

The aim of parametric studies is to show the sensitivity of the SIF to different electromagnetic boundary conditions on the crack for different materials. In Fig. 3-6 the normalized frequency is $\Omega = c\sqrt{\rho c_{44}^{-1}}\omega$.

In Fig. 3 the normalized SIF is plotted versus the normalized frequency for the piezoelectric material $BaTiO_3$. We see that the results for type II crack are close to the results for type IV and the results for type I are close to the results for type III.

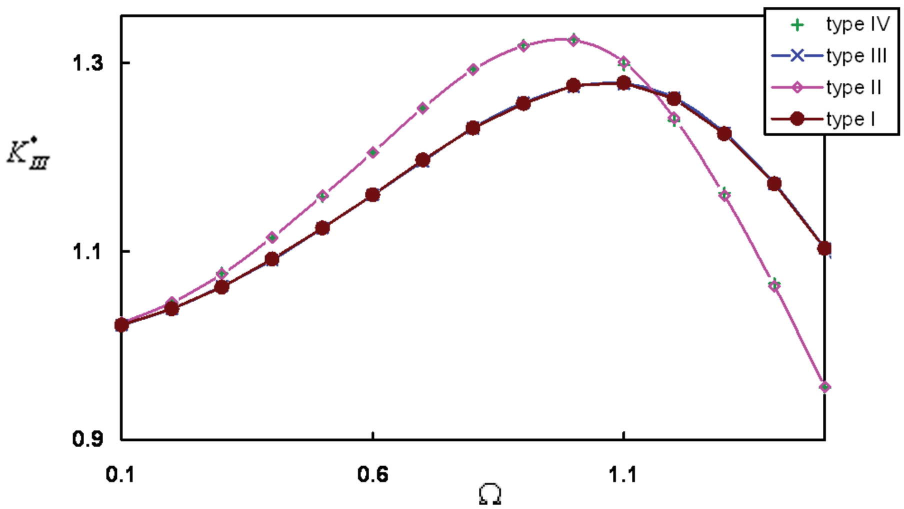

FIGURE 3. Normalized SIF versus the normalized frequency for different boundary conditions.

In Fig. 4 the normalized SIF is plotted versus the normalized frequency for piezomagnetic material $CoFe_2O_4$. We see close results for the considered four types of cracks.

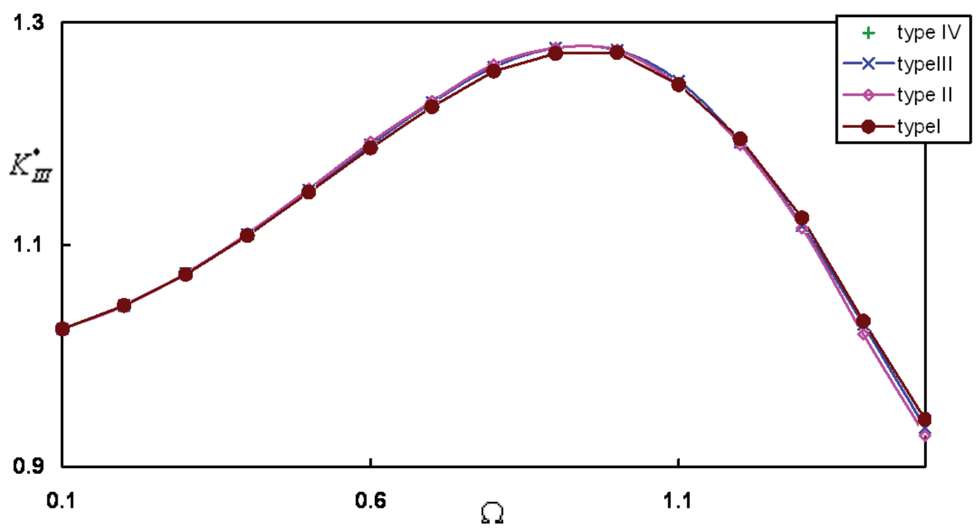

FIGURE 4. Normalized SIF versus the normalized frequency for different boundary conditions. The material is $CoFe_2O_4$.

In Fig. 5 the normalized SIF is plotted versus the normalized frequency for MEE composite. Similar to the results for $BaTiO_3$ we see that the results for type II crack are close to the results for type IV and the results for type I are close to the results for type III.

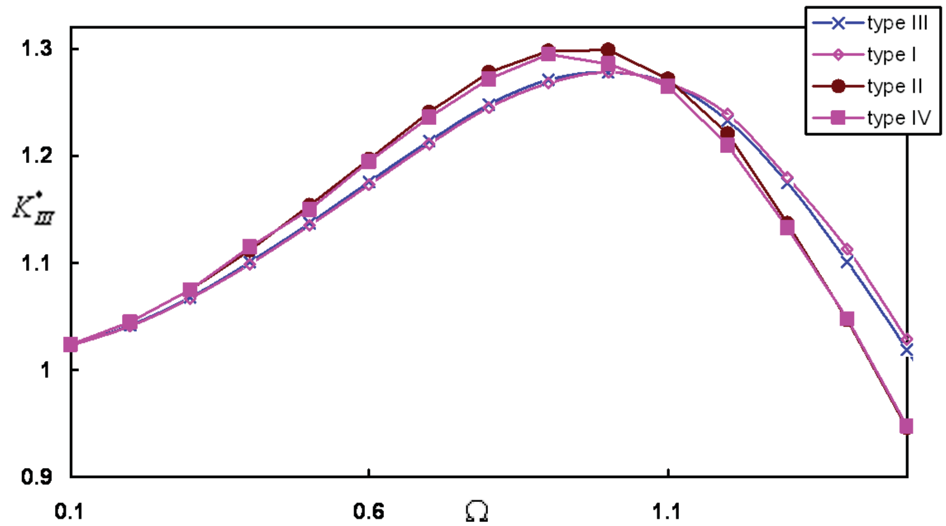

FIGURE 5. Normalized SIF versus the normalized frequency for different boundary conditions. The material is MEE composite.

In Fig. 6 the normalized SIF is plotted versus the normalized frequency for a branched crack. The crack is divided into 7BE. The angle between the right crack-tip element (the branched element) and the Ox_1 axis is $\delta = \frac{\pi}{4}$. The length of the branched lement is 0.75. The other BE are horizontal along the Ox_1 axis with the following coordinates: -5.0,-4.25,-3.25,-1.25,1.25,3.25,4.25. The material is MEE composite.

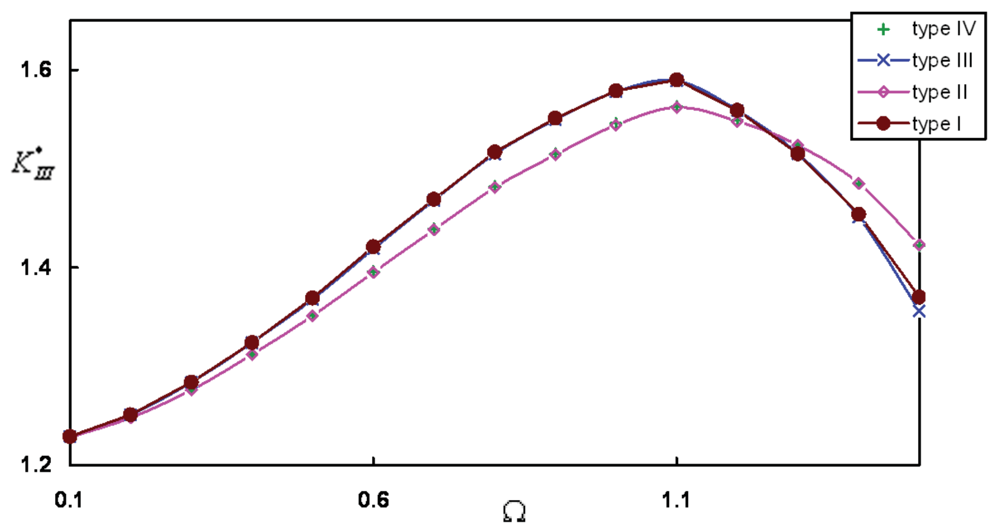

FIGURE 6. Normalized SIF versus the normalized frequency for a branched crack. The material is MEE composite.

5. Conclusions

The present work is focused on the boundary conditions for MEEM with antiplane cracks. As a solution method the BIEM is used. The parametric studies reveal the significant differences that may occur when using different boundary conditions. They also show that the electric boundary conditions have stronger influence on the SIF than the magnetic ones when we consider MEE composite or the piezoelectric material $BaTiO_3$.

Acknowledgements

The author acknowledges the support of BNSF under the grant DID 02/15.

References

1. Baolin Wang, Jiecai Han, "Discussion on electromagnetic crack face boundary conditions for the fracture mechanics of magneto-electro-elastic materials", *Acta Mech Sinica*, **22**(2006), 233-242.
2. Y. Benveniste," Magneto-Electric Effect in Fibrous Composites with Piezoelectric and Piezomagnetic Phases", *Physical Review B*, **51**(1995), 16424–16 427.
3. X. F. Li, "Dynamic analysis of a cracked magnetoelectroelastic medium under antiplane mechanical and inplane electric and magnetic impacts", *IJSS*, **42**(2005), 3185 – 3205.
4. Y. Stoynov, Tz. Rangelov, "Time harmonic crack problems in magnetoelectroelastic plane by BIEM", *Journal of Theoretical and Applied Mechanics*, **39**, (2009), 73–92.
5. G. R. Irwing, "Analysis of stress and strain near the end of a crack traversing a plate", *Journal of Applied Mechanics ASME*, **24**(1957), 361 – 364.
6. J. R. Rice, "A path independent integral and the approximate analysis of strain concentrations by notches and cracks", *J. Appl. Mech. ASME*, **35**(1968), 379-386.
7. C.-Y. Wang, Ch. Zhang, "3-D and 2-D Dynamic Green's Functions and Time-Domain BIEs for Piezoelectric Solids". *Eng. Anal. Bound. Elem.*, **29** (2005), 454–465.
8. Tsviatko Rangelov, Petia Dineva, Dietmar Gross, "Effects of material inhomogeneity on the dynamic behavior of cracked piezoelectric solids: a BIEM approach", *ZAMM · Z. Angew. Math. Mech.* **88**, (2008), 86 – 99.
9. Z.-G. Zhou, B. Wang, "Scattering of harmonic anti-plane shear waves by an interface crack in magneto-electro-elastic composites", *Applied Mathematics and Mechanics,* **26** (2005), 17-26.
10. F. Narita, Y. Shindo, "Dynamic Anti-Plane Shear of a Cracked Piezoelectric Ceramic", *Theoretical and Appl. Fract*. Mech., **29**(1998), 169–180.